

---

# Improving Uncertainty Estimates through the Relationship with Adversarial Robustness

---

Yao Qin   Xuezhi Wang   Alex Beutel   Ed H. Chi  
Google Research  
{yaoqin, xuezhw, alexbeutel, edchi}@google.com

## Abstract

Robustness issues arise in a variety of forms and are studied through multiple lenses in the machine learning literature. Neural networks lack *adversarial robustness* – they are vulnerable to adversarial examples that through small perturbations to inputs cause incorrect predictions. Further, trust is undermined when models give *miscalibrated* or *unstable* uncertainty estimates, i.e. the predicted probability is not a good indicator of how much we should trust our model and could vary greatly over multiple independent runs. In this paper, we study the connection between adversarial robustness, predictive uncertainty (calibration) and model uncertainty (stability) on multiple classification networks and datasets. We find that the inputs for which the model is sensitive to small perturbations (are easily attacked) are more likely to have poorly calibrated and unstable predictions. Based on this insight, we examine if calibration and stability can be improved by addressing those adversarially unrobust inputs. To this end, we propose Adversarial Robustness based Adaptive Label Smoothing (AR-AdaLS) that integrates the correlations of adversarial robustness and uncertainty into training by adaptively softening labels conditioned on how easily it can be attacked by adversarial examples. We find that our method, taking the adversarial robustness of the in-distribution data into consideration, leads to better calibration and stability over the model even under distributional shifts. In addition, AR-AdaLS can also be applied to an ensemble model to achieve the best calibration performance.

## 1 Introduction

The robustness of machine learning algorithms is becoming increasingly important as ML systems are being used in higher-stakes applications. However, “robustness” is often used informally and has been widely studied from varied perspectives in the machine learning literature. In one line of research, neural networks are shown to lack *adversarial robustness* – small perturbations to the input can successfully fool classifiers into making incorrect predictions [31, 7, 4, 19, 24]. In largely separate lines of work, researchers have studied uncertainty in model’s predictions. For example, models are often *miscalibrated* where the predicted confidence is not indicative of the true likelihood of the model being correct [8, 32, 16, 33, 15]. Further, these uncertainty estimates are often *unstable*, with independent training runs resulting in significant differences in the predictions [26, 18, 22, 38]. Both of these uncertainty issues are exacerbated when models are asked to make predictions on data different from the training distribution [27], which becomes an issue in practical settings where it is important that we can trust model predictions even under distributional shift. Taken together, we see a significant challenge for trusting model predictions – models often misrepresent confidence in their predictions and are overly sensitive to spurious changes in input, training, or distribution.

Despite robustness, in all its forms, being a popular area of research, the *relationship* among these perspectives has not been extensively explored previously. In this paper, we study the correlation

between adversarial robustness and calibration as well as model’s stability. We discover that input data that are sensitive to small adversarial perturbations (are easily attacked) are more likely to have poorly calibrated and unstable predictions. This holds true on a number of network architectures for classification and on all the datasets that we consider: SVHN [21], CIFAR-10 [14], CIFAR-100 [14] and ImageNet [25]. This suggests that the miscalibrated and unstable uncertainty estimates on those adversarially unrobust data greatly degrades the performance of a model’s calibration and stability. Based on this insight, we hypothesize and study if calibration and stability, particularly on unknown shifted data, can be improved by giving different supervision to the model depending on adversarial robustness of each training data.

To this end, we propose **Adversarial Robustness based Adaptive Label Smoothing (AR-AdaLS)** that integrates the correlations of adversarial robustness and uncertainty into training by adaptively smoothing the training labels conditioned on how unrobust an input is. Our method improves label smoothing [31] by explicitly teaching the model to differentiate the training data according to their adversarial robustness and then adaptively smooth their labels. By giving different supervision to the training data, our method leads to better calibration and stability over the model without an increase of latency during inference. In particular, since adversarially unrobust data can be considered as an outlier of the underlying data distribution [2], our method, by taking the adversarial robustness of the in-distribution data into consideration during training, can even greatly improve model’s calibration and stability on held-out shifted data, whose distribution is different from the training distribution. Lastly, we propose “AR-AdaLS of Ensemble” to combine our AR-AdaLS and deep ensembles [16], which is the state-of-the-art method especially under distributional shift [27], to further improve the calibration performance for shifted data.

In summary, our main contributions are as follows:

- **Relationship among Robustness Metrics:** By exploring three metrics for adversarial robustness, predictive uncertainty (calibration) and model uncertainty (stability), we find a significant correlation between adversarial robustness and uncertainty estimates: inputs that are unrobust to adversarial attacks are more likely to have poorly calibrated and unstable predictions.
- **Algorithm:** We hypothesize that training a model with different supervision based on adversarial robustness of each input will make the model better calibrated and more stable. To this end, we propose AR-AdaLS to automatically learn how much to soften the labels of training data based on their adversarial robustness. Further, we introduce “AR-AdaLS of Ensemble” to show how to apply AR-AdaLS to an ensemble model.
- **Experimental Analysis:** On CIFAR-10 and ImageNet, we find that AR-AdaLS is more effective than previous label smoothing methods in improving calibration and stability, particularly for shifted data. Further, we find that while ensembling can be beneficial, applying AR-AdaLS to adaptively calibrate ensembles offers further improvements to the model’s uncertainty estimates.

## 2 Related Work

**Uncertainty Estimates** How to better estimate a model’s predictive uncertainty is an important research topic, since many models with a focus on accuracy may fall short in predictive uncertainty. A popular way to improve a model’s predictive uncertainty is to make the model well-calibrated, e.g., post-hoc calibration by temperature scaling [8], and multiclass Dirichlet calibration [15]. In addition, dropout-based variational inference [5, 13] can help DNN models make less over-confident predictions and be better calibrated. Recently, mixup training [37] has been shown to improve both models’ generalization and calibration [32], by preventing the model from being over-confident in its predictions. Despite the success of improving uncertainty estimates over in-distribution data, [27] argue that it does not usually translate to a better performance on data that shift from the training distribution. Among all the methods evaluated by [27] under distributional shift, ensemble of deep neural networks [16], is shown to be most robust to dataset shift, producing the best uncertainty estimates, especially on the shifted data.

**Adversarial Robustness** On the other hand, machine learning models are known to be brittle [34] and vulnerable to adversarial examples [1, 3, 4, 11]. Many defenses have been proposed to improve model’s adversarial robustness [28, 35, 6], however are further attacked by more advanced defense-aware attacks [4, 1]. Recently, [2, 29] defines adversarial robustness as the minimum distance in

Table 1: Network architecture and accuracy used for each dataset.

Dataset	SVHN	CIFAR-10	CIFAR-100	ImageNet
Network	CNN-7	ResNet-29 v2 [10]	Wide ResNet-28-10 v2 [36]	ResNet-101 v1 [9]
Accuracy	95.0%	91.4%	79.4%	77.7%

the input domain required to change the model’s output prediction by constructing an adversarial attack. The most recent work that is close to ours, [2], makes the interesting observation that easily attackable training or testing examples are often outliers in the underlying data distribution and then use adversarial robustness to determine an improved ordering for curriculum learning. Our work, instead, explores the relationship between adversarial robustness and calibration as well as stability. In addition, we use adversarial robustness as an indicator to adaptively smooth the training labels in order to improve model’s calibration and stability.

**Label Smoothing** Label smoothing is originally proposed in [30] and is shown to be effective in improving the quality of uncertainty estimates in [20, 32]. Instead of training a network by minimizing the cross-entropy loss between the predicted probability  $\hat{p}$  and the one-hot label  $p$ , label smoothing minimizes the cross-entropy between the predicted probability and a softened label  $\tilde{p} = p(1 - \epsilon) + \frac{\epsilon}{Z}$ , where  $Z$  is the number of classes in the dataset and  $\epsilon$  is a hyperparameter which controls the degree of the smoothing effect. Our work makes label smoothing adaptive and incorporates adversarial robustness to further improve calibration and stability.

### 3 Metrics for adversarial robustness and uncertainty

In this section, we introduce three metrics to measure different aspects of a model’s robustness. We use arrows to indicate which direction is better.

**Adversarial robustness**  $\uparrow$  Adversarial robustness measures the minimum distance in the input domain required to change the model’s output prediction by constructing an adversarial attack [2, 29]. Specifically, given an input  $x$  and a classifier  $f(\cdot)$  that predicts the class for the input, the adversarial robustness is defined as the minimum adversarial perturbation  $\delta$  that enables  $f(x + \delta) \neq f(x)$ . Following the work [2], we construct the  $\ell_2$  based CW attack [4] and then use the  $\ell_2$  norm of the adversarial perturbation  $\|\delta\|_2$  to measure the distance to the decision boundary. Therefore, a more adversarially robust input requires a larger adversarial perturbation to change the model’s prediction.

**Calibration metric**  $\downarrow$  Model’s calibration measures the alignment between the predicted probability and the accuracy. Well calibrated uncertainty estimates convey the information about how much we should trust a model’s prediction. We follow the widely used expected calibration error (**ECE**) to measure the calibration performance of a network [8, 27]. To compute the ECE, we need to first divide all the data into  $K$  buckets sorted by their predicted probability (confidence) of the predicted class. Let  $B_k$  represent the set of data in the  $k$ -th confidence bucket. Then the accuracy and the confidence of  $B_k$  are defined as  $\text{acc}(B_k) = \frac{1}{|B_k|} \sum_{i \in B_k} \mathbf{1}(\hat{y}_i = y_i)$  and  $\text{conf}(B_k) = \frac{1}{|B_k|} \sum_{i \in B_k} \hat{p}_i^{\hat{y}_i}$ , where  $\hat{y}$  and  $y$  represent the predicted class and the true class respectively, and  $\hat{p}^{\hat{y}}$  is the predicted probability of  $\hat{y}$ . The ECE is then defined as  $\text{ECE} = \sum_{k=1}^K \frac{|B_k|}{N} |\text{acc}(B_k) - \text{conf}(B_k)|$ , where  $N$  is the number of the data. A better calibrated model should have a smaller ECE.

**Model uncertainty metric**  $\downarrow$  Follow the work in [18, 22], we estimate the model uncertainty by computing the variance of  $M$  independently trained models with random initializations. The variance is computed as  $\sigma^2 = \frac{1}{M-1} \frac{1}{N} \sum_{m=1}^M \sum_{i=1}^N (\hat{p}_{m,i} - \bar{p}_i)^2$ , where  $\hat{p}_{m,i}$  is the  $m$ -th model’s predicted probability of the  $i$ -th data and  $\bar{p}_i = \frac{1}{M} \sum_{m=1}^M \hat{p}_{m,i}$  is the average predicted probability over  $M$  runs. In addition, the variance can also be used to measure the model’s stability, where the most stable model has the smallest variance.

### 4 Correlations between adversarial robustness and uncertainty estimates

Although these metrics of adversarial robustness and uncertainty estimates are conceptually related, they are measuring quite different properties: As we can see that the adversarial robustness measures

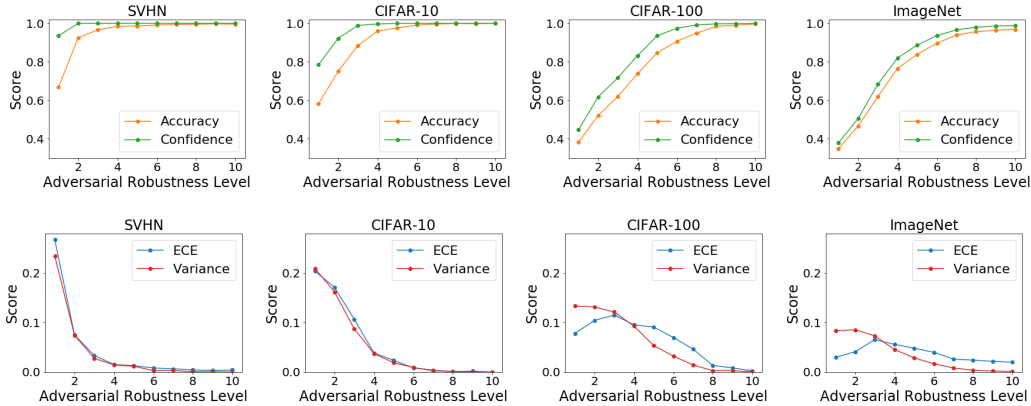


Figure 1: Correlations between adversarial robustness and uncertainty estimates on the clean test set on SVHN, CIFAR-10, CIFAR-100 and ImageNet. **Top:** Accuracy and confidence score of the predicted class. **Bottom:** ECE and variance score (lower is better) in each adversarial robustness subset. The higher the adversarial robustness level is, the more adversarially robust (harder to attack) the data are.

the property of the data by computing the adversarial perturbation  $\delta$  from the input domain, while the metrics for calibration and stability depend mainly on the model’s predicted probability in the output space.

To test if there is any correlation between adversarial robustness and uncertainty estimates, we perform experiments on the clean test set across four classification datasets: SVHN [21], CIFAR-10 [14], CIFAR-100 [14] and ImageNet [25] with different networks, whose architecture and accuracy are shown in Table 1. We refer to these models as “Vanilla” for each dataset in the following discussion. Note that there are 10 classes for SVHN and CIFAR-10, 100 classes for CIFAR-100 and 1000 classes for ImageNet. The details for training each vanilla network are included in Section A in the Appendix.

#### 4.1 Adversarial robustness and calibration

To explore the relationship between adversarial robustness and calibration, we start with the relationship between adversarial robustness and confidence together with accuracy. Specifically, we rank the input data according to their adversarial robustness and then divide the dataset into  $R$  equally-sized subsets ( $R = 10$  used in this paper). For each adversarial robustness subset, we compute the accuracy and the average confidence score of the predicted class. As shown in the first row in Figure 1, we can clearly see that both accuracy and confidence increase as adversarial robustness of the input data, and confidence is consistently higher than accuracy in each adversarial robustness subset across four datasets. This indicates that although vanilla classification models achieve the state-of-the-art accuracy, they tend to give over-confident predictions, especially for those unrobust data.

Based on this, to explore the relationship between adversarial robustness and calibration, we compute the expected calibration error (ECE) in each adversarial robustness subset, shown in the bottom row of Figure 1. In general, we find that those unrobust data in lower adversarial robustness levels are more likely to be over-confident and less well calibrated (larger ECE). For more robust examples, there is a better alignment between their confidence and accuracy, and the ECE over those examples is close to 0. On larger-scale ImageNet, while we still see the general trend that less robust examples are less well calibrated, we see that the least robust examples are relatively well calibrated. We hypothesize this may be due to larger data and less overfitting.

#### 4.2 Adversarial robustness and stability

Furthermore, we also find a strong correlation between adversarial robustness and model stability across multiple independent runs. As shown in the bottom row of Figure 1, we see that those adversarially unrobust examples tend to have a much higher variance compared to the robust across all four datasets. The strong alignment between the adversarial robustness of the input data and the

stability of their predictions suggests that in order to improve a model’s overall stability, one should target to reduce the variance of those unrobust, easily attacked data.

Both of these results are surprising as they are connecting very different concepts. In particular, adversarial robustness is measured over the input domain while both calibration and stability are measured over the output space. Given the strong empirical connection, we now ask: can we improve model calibration and stability by targeting adversarially unrobust examples?

## 5 Adversarial robustness based adaptive label smoothing

Based on the correlation between adversarial robustness and uncertainty estimates, we hypothesize and study if calibration and stability can be improved by giving different supervision to the model depending on the adversarial robustness of each training data. To this end, we propose a method named **Adversarial Robustness based Adaptive Label Smoothing (AR-AdaLS)**, which adapts label smoothing conditional on adversarial robustness.

### 5.1 Adversarial robustness based label smoothing

Inspired by the correlations between adversarial robustness and uncertainty estimates discussed in Section 4, we perform label smoothing at different degrees to the training data based on their adversarial robustness. Specifically, we sort and divide the training data into  $R$  small subsets with equal size according to their adversarial robustness<sup>1</sup> and then use  $\epsilon_r$  to soften the labels in each training subset  $S_r^{train}$ . The soft labels can be formulated as:

$$\tilde{p}_r = p_r(1 - \epsilon_r) + \frac{\epsilon_r}{Z}, \tag{1}$$

where  $p_r^{z=y} = 1$  for the correct class  $y$  and  $p_r^{z \neq y} = 0$  for the others,  $p_r$  stands for the one-hot label, and  $Z$  is the number of classes in the dataset. The parameter  $\epsilon_r$  controls the degree of smoothing effect and allows for different levels of smoothing in each adversarial robustness subset. Generally, a relatively larger  $\epsilon_r$  is desirable for lower adversarial robustness levels such that the model learns to make a lower confidence prediction. Instead of empirically setting the parameter  $\epsilon_r$  in each adversarial robustness subset, we allow it to be adaptively updated according to the calibration performance on the validation set (discussed in Section 5.2). In this way, we explicitly train a network with different supervision based on the adversarial robustness of training data.

There are two options to obtain the adversarial robustness. One is “on the fly”: to keep creating the adversarial attacks during training, which provides precise adversarial robustness ranking but at the cost of great computing time. The other is to “pre-compute” the adversarial robustness by attacking a vanilla model with the same network architecture but trained with the hard labels. This is more efficient but at the sacrifice of the precision of adversarial robustness ranking. In practice, we find that it is sufficient to make the network differentiate the robust and unrobust data with the pre-computed adversarial robustness. Therefore, we use the pre-computed adversarial robustness for our experiments.

### 5.2 Adaptive learning mechanism

To find the best hyperparameter  $\epsilon$  for label smoothing, previous methods [30, 32] sweep  $\epsilon$  in a range and choose the one that has the best validation performance. However, in our setting, the number of combinations of  $\epsilon_r$  increases exponentially with the number of adversarial robustness subsets  $R$ . To this end, we propose an adaptive learning mechanism to automatically learn the parameter  $\epsilon_r$  in each adversarial robustness subset. The overall training procedure is summarized in Algorithm 1.

First, we denote the soft label for the correct class in the  $r$ -th adversarial robustness subset as  $\tilde{p}_r^{z=y}$ . According to Eqn. (1), we can derive:

$$\tilde{p}_r^{z=y} = 1 - \epsilon_r + \frac{\epsilon_r}{Z}. \tag{2}$$

Since well-calibrated uncertainty estimates should be aligned with the empirical accuracy, we use the calibration performance in the *validation set* to help update  $\tilde{p}_r^{z=y}$  for the *training data*. Specifically,

<sup>1</sup>Note, this method could be easily adapted to conditioning on other attributes of data.

---

**Algorithm 1** Pseudocode of the training procedure for AR-AdaLS

---

**Input:** number of classes  $Z$ , number of training epochs  $T$ , number of adversarial robustness subset  $R$ , learning rate of adaptive label smoothing  $\alpha$ .

For each adversarial robustness training subset, we initialize the soft label as the one-hot label  $\tilde{p}_{r,t} = p_r$ , and initialize the soft label for the correct class  $\tilde{p}_{r,t}^{z=y} = 1$ .

**for**  $t = 1$  **to**  $T$  **do**

    Minimize cross-entropy loss between soft label and predicted probability  $\frac{1}{R} \sum_r \mathcal{L}(\tilde{p}_{r,t}, \hat{p}_{r,t})$

**for**  $r = 1$  **to**  $R$  **do**

        Update  $\tilde{p}_{r,t}^{z=y} \leftarrow \tilde{p}_{r,t}^{z=y} - \alpha \cdot \{\text{conf}(S_r^{val})_t - \text{acc}(S_r^{val})_t\}$  ▷ according to Eqn. (3)

        Clip  $\tilde{p}_{r,t}^{z=y}$  to be within  $(\frac{1}{Z}, 1]$

        Update  $\epsilon_{r,t} \leftarrow (\tilde{p}_{r,t}^{z=y} - 1) \cdot \frac{Z}{1-Z}$  ▷ according to Eqn. (4)

        Update  $\tilde{p}_{r,t} \leftarrow p_r(1 - \epsilon_{r,t}) + \frac{\epsilon_{r,t}}{Z}$  ▷ according to Eqn. (1)

**end for**

**end for**

---

we first rank the adversarial robustness of the validation data and split the validation set into  $R$  equally-sized subsets. Then, we use the difference between confidence and accuracy in the  $r$ -th adversarial robustness validation subset  $\text{conf}(S_r^{val}) - \text{acc}(S_r^{val})$  to update the soft label for the correct class of training data in the  $r$ -th adversarial robustness training subset  $S_r^{train}$ ,

$$\tilde{p}_{r,t+1}^{z=y} = \tilde{p}_{r,t}^{z=y} - \alpha \cdot \{\text{conf}(S_r^{val})_t - \text{acc}(S_r^{val})_t\} \quad (3)$$

where  $\tilde{p}_{r,t}^{z=y}$  is the soft label of the correct class in the  $r$ -th adversarial robustness training subset at time step  $t$ . The accuracy and the confidence of  $S_r^{val}$  are defined as  $\text{acc}(S_r^{val}) = \frac{1}{|S_r^{val}|} \sum_{i \in S_r^{val}} \mathbf{1}(\hat{y}_i = y_i)$  and  $\text{conf}(S_r^{val}) = \frac{1}{|S_r^{val}|} \sum_{i \in S_r^{val}} \hat{p}_i^{z=\hat{y}_i}$ , where  $\hat{y}$  and  $y$  is the predicted class and the true class respectively,  $\hat{p}^{z=\hat{y}}$  denotes the the predicted probability of the predicted class. The hyperparameter  $\alpha > 0$  plays a role as a learning rate to update the soft label  $\tilde{p}_{r,t}^{z=y}$  based on the difference between the predicted confidence and accuracy in the validation set. Intuitively, if we assign a large  $\tilde{p}_{r,t}^{z=y}$  to training data, then the network tends to make a high confidence prediction and vice versa. Therefore, if the confidence is greater than the accuracy ( $\text{conf}(S_r^{val}) > \text{acc}(S_r^{val})$ ) in the validation set, we should reduce  $\tilde{p}_{r,t}^{z=y}$  to teach the network to be less confident. Otherwise, we should increase  $\tilde{p}_{r,t}^{z=y}$ . In addition, we also need to constrain  $\tilde{p}_{r,t}^{z=y}$  to be within  $(\frac{1}{Z}, 1]$  after each update as it stands for the true probability of the correct class, where  $Z$  is the number of classes in the dataset.

For a given  $\tilde{p}_{r,t}^{z=y}$ , we can easily obtain  $\epsilon_r$  by reversing Eqn. (2):

$$\epsilon_r = (\tilde{p}_{r,t}^{z=y} - 1) \cdot \frac{Z}{1-Z}, \quad (4)$$

and the soft labels for all the classes  $\tilde{p}_r$  can be computed according to Eqn. (1). We update the soft labels after each training epoch in our experiments.

Note that this adaptive learning mechanism can be easily applied to standard label smoothing without adversarial robustness slicing ( $R = 1$ ). In this case, we can replace sweeping the hyperparameter  $\epsilon$  with this adaptive learning method, named as “**Adaptive Label Smoothing**” (**AdaLS**). Our proposed AdaLS and AR-AdaLS does not increase the inference time: we test AdaLS and AR-AdaLS exactly the same as a vanilla model.

## 6 Experiments

We now test our methods on both clean and shifted data for CIFAR-10 and ImageNet for calibration and stability. The shifted dataset [12] consists of different types (19 types for CIFAR-10 and 15 types for ImageNet) of corruptions, e.g., noise, blur, weather and digital categories that are frequently encountered in natural images. Each type of corruption has five levels of shift intensity, with higher levels having more corruption. For each shift intensity, we report the results with a box plot summarizing the 25th, 50th, 75th quartiles across the types of shift. We first test single-model approaches and then explore how our methods compose with deep ensembles [16].

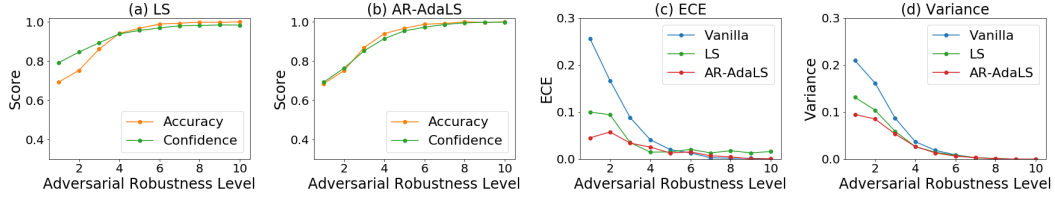


Figure 2: Comparison between LS and our AR-AdaLS on the clean test set of CIFAR-10. **(a)** and **(b)**: Accuracy and confidence score of the predicted class in each adversarial robustness subset. **(c)** and **(d)**: ECE and variance score of Vanilla, LS and AR-AdaLS.

## 6.1 Baselines

We compare our proposed **AR-AdaLS** with the following methods:

- Vanilla: We train a ResNet29-v2 [10] for CIFAR-10 and a ResNet101-v1 [9] for ImageNet with regular training mechanism that one-hot labels are used for cross-entropy loss.
- Ensemble of Vanilla [16]: Ensemble of  $M$  vanilla models independently trained with random initialization ( $M = 5$  in our experiments). Deep ensembles are shown to be the best method for model’s calibration, especially under distributional shift [27].
- Label Smoothing (**LS**) [30]: smooth the hard labels to soft labels and sweep the hyperparameter  $\epsilon$  which controls the smoothing degree in a range to find the best hyperparameter  $\epsilon$ .
- Adaptive Label Smoothing (**AdaLS**): we use our proposed adaptive learning mechanism introduced in Section 5.2 to automatically learn the hyperparameter  $\epsilon$  rather than sweeping to find the best  $\epsilon$ .

We train all the methods with the same network architectures and keep all the training hyperparameters to be the same: e.g., learning rate, batch size, number of training epochs, for fair comparison. Please refer to Appendix for all the training details and hyperparameters.

## 6.2 Visualization of improvement over uncertainty estimates

Since our proposed AR-AdaLS is built upon label smoothing (LS), in Figure 2 we visualize the effect of label smoothing (LS) and our AR-AdaLS. Comparing Figure 2 (a) and (b), we can clearly see that AR-AdaLS is better at calibrating the data than label smoothing, especially on the unrobust examples (lower adversarial robustness level). Further, we show plots of ECE and variance in Figure 2 (c) and (d). Both label smoothing and AR-adaLS improve model’s calibration and uncertainty over vanilla model and AR-AdaLS has the best performance among three methods. This suggests that AR-AdaLS is better at improving calibration and stability in unrobust regions, not just on average.

Figure 3 summarizes the ECE and variance for CIFAR-10 and ImageNet for both clean and shifted data with different levels of corruptions [12]. Since ensembles are used to compute the variance (as discussed in Section 3), we only report the variance of single-model based methods. On the clean test set, all non-vanilla methods achieve comparable low values of ECE, and AR-AdaLS has the best performance in improving model’s stability by having the smallest variance.

**Generalization over shifted dataset** When the intensity of shift increases, AR-AdaLS significantly outperforms other single-model based methods with the lowest ECE and variance. Contrasting with LS and AdaLS, we see AR-AdaLS benefits greatly from the adversarial robustness slicing. As a result, our model learns to give smaller soft labels of the correct class to those adversarially unrobust training data, which can also be considered as outliers of the underlying data distribution [2]. Therefore, when tested on the shifted data that deep networks have been shown to produce pathologically over-confident predictions [12], our model correctly learns to make a relatively lower confidence prediction, resulting in a better calibration performance. When we compare to an ensemble of *five* Vanilla models, we can see that AR-AdaLS achieves comparable calibration performance on CIFAR-10 and the ensemble is better under highly shifted data on ImageNet.

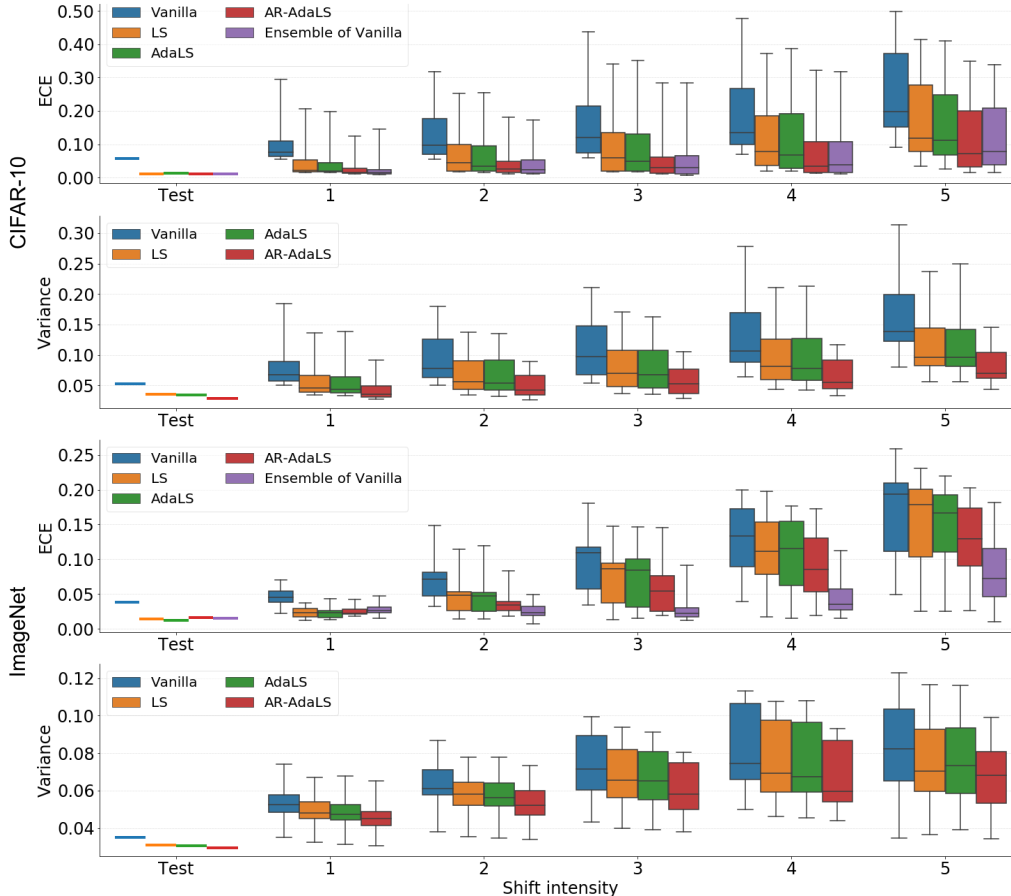


Figure 3: ECE and variance on clean test and shifted data on CIFAR-10 and ImageNet. For each shift intensity, we show the results with a box plot summarizing the 25th, 50th, 75th quartiles across 19 shift types on CIFAR10-C and 15 shift types on ImageNet-C. The error bars indicate the *min* and *max* value across different shift types. Accuracy figures are shown in Appendix that all the single-model based methods have comparable accuracy while ensembles achieve higher accuracy.

### 6.3 Combination with deep ensembles

In this section, we discuss if the two best models: deep ensembles and our AR-AdaLS are complementary to each other. To this end, we propose the following two ways to combine them:

**Ensemble of AR-AdaLS:** As in [16, 17], we ensemble AR-AdaLS by training multiple independent AR-AdaLS models with random initialization, and average their predictions at inference.

**AR-AdaLS of Ensemble:** Instead of computing soft labels independently for each AR-AdaLS model, we perform AR-AdaLS on the ensembled predictions, i.e., in Eqn. (3) we compute confidence and accuracy based on the average of the  $M$  model predictions. Each model is then supervised with the same soft labels. We will see this slight distinction in training is quite important.

**Discussion** We present the results for CIFAR-10 in Figure 4. At a high level, we see that AR-AdaLS of Ensemble performs the best across both clean test data and all intensities of shifted data (numerical results are provided in Table 3 in Appendix). Looking more closely, some trends emerge: all of the ensemble methods perform relatively well for highly shifted data (intensity 4–5), but Ensemble of AR-AdaLS performs much worse on less shifted and clean test data. Digging deeper we display the confidence of the predicted class and accuracy of each single model and the corresponding ensemble models on the clean test set of CIFAR-10 and ImageNet in Figure 5. We can clearly see that the ensemble models generally increase accuracy and decrease confidence compared to a single

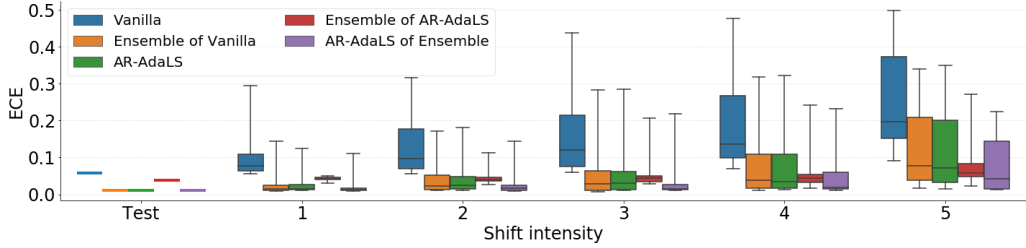


Figure 4: Comparison of ensembled models: ECE on both clean test data and shifted data on CIFAR-10 dataset. For each intensity of shift, we show the results with a box plot summarizing the 25th, 50th, 75th quartiles across 19 types of shift in CIFAR10-C dataset. The error bars indicate the min and max value across different shift types. The accuracy figure is shown in Appendix. All the ensemble models have a relatively higher accuracy than single-model based methods.

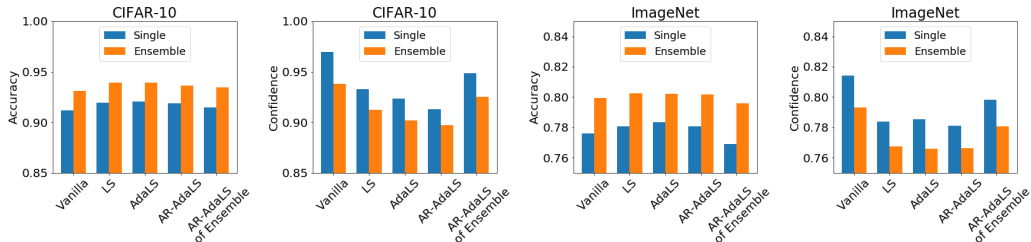


Figure 5: Comparing accuracy and confidence of the predicted class between single model and the corresponding ensemble model for each method.

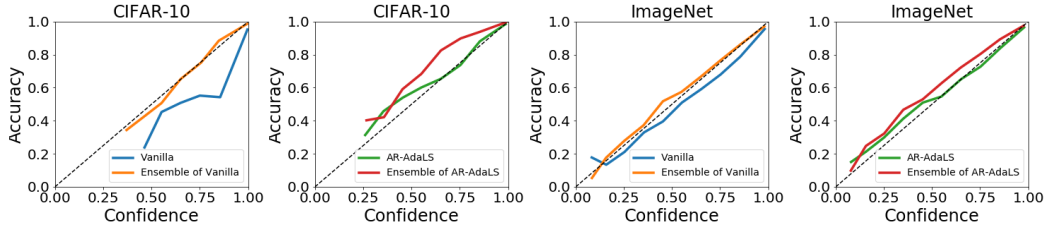


Figure 6: Reliability diagram of accuracy versus confidence of single model and ensemble model on the clean test of CIFAR-10 and ImageNet. The perfect calibrated model should be aligned with the diagonal dotted line (above is under-confident, below is over-confident).

model, which results from the disagreement of the prediction of each single model in ensembles. Therefore, naive deep ensembles can improve calibration on highly shifted data where single-model is over-confident but can harm calibration if applied to a well-calibrated single-model. This is made clearer in Figure 6: while deep ensembles make over-confident vanilla model well calibrate, it leads the well calibrated AR-AdaLS models to be under-confident (similar patterns observed on LS and AdaLS, shown in Figure 8 in Appendix). From this perspective, AR-AdaLS of Ensemble avoids this issue by adaptively adjusting smoothing to keep the ensemble well calibrated. Taken together we see that AR-AdaLS improves calibration and stability for both single-models and ensembles.

## 7 Conclusion

In this paper, we have explored the correlations between adversarial robustness and calibration as well as stability. We find across multiple datasets that adversarially unrobust (easily attacked) data are more likely to have poorly calibrated and unstable predictions. Based on this insight, we propose AR-AdaLS to adaptively smooth the labels of the training data based on their adversarial robustness. In our experiments we see that AR-AdaLS is more effective than previous label smoothing methods in improving calibration and stability, particularly for shifted data, and can offer improvements on top of already strong ensembling methods. We believe this is an exciting new use for adversarial robustness as a means to more generally improve model trustworthiness, not just by limiting adversarial attacks but also improving uncertainty on unexpected data. We hope this spurs further work at the intersections of these areas of research.

## Broader Impact

The robustness of model accuracy and uncertainty estimates, to both clean and out-of-distribution data, is increasingly understood to be critical to trusting machine learning in high-stakes applications. For example, for determining if a person is diagnosed with a certain disease based on medical imaging, in addition to model’s high accuracy overall, the model should also give *responsible* uncertainty estimates in terms of not being over-confident under cases where it should not be (e.g., people with special health conditions might have out-of-distribution imaging results). For auto-driving applications it is also important for the model to give low uncertainty estimates over unseen data, which could save lives.

This work aims to utilize adversarial robustness to improve uncertainty estimates in ML models. We believe improving these metrics are beneficial to the applications above. While our method by no means fully solves these concerns, we hope this research both raise people’s awareness of the importance of these metrics and encourages further improvements to the trustworthiness of real-world ML models.

## References

- [1] A. Athalye, N. Carlini, and D. Wagner. Obfuscated gradients give a false sense of security: Circumventing defenses to adversarial examples. In *International Conference on Machine Learning*, 2018.
- [2] N. Carlini, Ú. Erlingsson, and N. Papernot. Distribution density, tails, and outliers in machine learning: Metrics and applications. *ArXiv*, abs/1910.13427, 2019.
- [3] N. Carlini and D. Wagner. Adversarial examples are not easily detected: Bypassing ten detection methods. In *Proceedings of the 10th ACM Workshop on Artificial Intelligence and Security, AISec ’17*, page 3–14, New York, NY, USA, 2017. Association for Computing Machinery.
- [4] N. Carlini and D. Wagner. Towards evaluating the robustness of neural networks. In *2017 IEEE Symposium on Security and Privacy (SP)*, pages 39–57. IEEE, 2017.
- [5] Y. Gal and Z. Ghahramani. Dropout as a bayesian approximation: Representing model uncertainty in deep learning. In *International Conference on Machine Learning*, pages 1050–1059, 2016.
- [6] I. Goodfellow, Y. Qin, and D. Berthelot. Evaluation methodology for attacks against confidence thresholding models. 2018.
- [7] I. Goodfellow, J. Shlens, and C. Szegedy. Explaining and harnessing adversarial examples. In *International Conference on Learning Representations*, 2014.
- [8] C. Guo, G. Pleiss, Y. Sun, and K. Q. Weinberger. On calibration of modern neural networks. In *International Conference on Machine Learning*, 2017.
- [9] K. He, X. Zhang, S. Ren, and J. Sun. Deep residual learning for image recognition. In *Proceedings of the IEEE conference on Computer Vision and Pattern Recognition*, pages 770–778, 2016.
- [10] K. He, X. Zhang, S. Ren, and J. Sun. Identity mappings in deep residual networks. In *European Conference on Computer Vision*, pages 630–645. Springer, 2016.
- [11] W. He, B. Li, and D. Song. Decision boundary analysis of adversarial examples. In *International Conference on Learning Representations*, 2018.
- [12] D. Hendrycks and T. G. Dietterich. Benchmarking neural network robustness to common corruptions and perturbations. *International Conference on Learning Representations*, 2019.
- [13] D. P. Kingma, T. Salimans, and M. Welling. Variational dropout and the local reparameterization trick. In *Advances in Neural Information Processing Systems*, pages 2575–2583, 2015.
- [14] A. Krizhevsky. Learning multiple layers of features from tiny images. Technical report, University of Toronto, 2009.
- [15] M. Kull, M. Perello Nieto, M. Kängsepp, T. Silva Filho, H. Song, and P. Flach. Beyond temperature scaling: Obtaining well-calibrated multi-class probabilities with dirichlet calibration. In *Advances in Neural Information Processing Systems 32*, pages 12316–12326, 2019.

- [16] B. Lakshminarayanan, A. Pritzel, and C. Blundell. Simple and scalable predictive uncertainty estimation using deep ensembles. In *Advances in Neural Information Processing Systems*, page 6405–6416. Curran Associates Inc., 2017.
- [17] S. Lee, S. Purushwalkam, M. Cogswell, D. Crandall, and D. Batra. Why m heads are better than one: Training a diverse ensemble of deep networks. *arXiv preprint arXiv:1511.06314*, 2015.
- [18] A. Loquercio, M. Segù, and D. Scaramuzza. A general framework for uncertainty estimation in deep learning. *IEEE Robotics and Automation Letters*, 5:3153–3160, 2019.
- [19] A. Madry, A. Makelov, L. Schmidt, D. Tsipras, and A. Vladu. Towards deep learning models resistant to adversarial attacks. In *International Conference on Learning Representations*, 2017.
- [20] R. Müller, S. Kornblith, and G. E. Hinton. When does label smoothing help? In *Advances in Neural Information Processing Systems*, pages 4694–4703, 2019.
- [21] Y. Netzer, T. Wang, A. Coates, A. Bissacco, B. Wu, and A. Y. Ng. Reading digits in natural images with unsupervised feature learning. In *NIPS workshop on deep learning and unsupervised feature learning*, volume 2011, page 5, 2011.
- [22] T. Pearce, A. Brintrup, M. Zaki, and A. Neely. High-quality prediction intervals for deep learning: A distribution-free, ensembled approach. In *International Conference on Machine Learning*, 2018.
- [23] Y. Qin, N. Frosst, C. Raffel, G. Cottrell, and G. Hinton. Deflecting adversarial attacks. *arXiv preprint arXiv:2002.07405*, 2020.
- [24] Y. Qin, N. Frosst, S. Sabour, C. Raffel, G. Cottrell, and G. Hinton. Detecting and diagnosing adversarial images with class-conditional capsule reconstructions. *International Conference on Learning Representations*, 2020.
- [25] O. Russakovsky, J. Deng, H. Su, J. Krause, S. Satheesh, S. Ma, Z. Huang, A. Karpathy, A. Khosla, M. S. Bernstein, A. C. Berg, and F.-F. Li. Imagenet large scale visual recognition challenge. *International Journal of Computer Vision*, 115:211–252, 2015.
- [26] L. Ruthotto and E. Haber. Deep neural networks motivated by partial differential equations. *Journal of Mathematical Imaging and Vision*, pages 1–13, 2019.
- [27] J. Snoek, Y. Ovadia, E. Fertig, B. Lakshminarayanan, S. Nowozin, D. Sculley, J. Dillon, J. Ren, and Z. Nado. Can you trust your model’s uncertainty? evaluating predictive uncertainty under dataset shift. In *Advances in Neural Information Processing Systems*, pages 13969–13980, 2019.
- [28] Y. Song, T. Kim, S. Nowozin, S. Ermon, and N. Kushman. Pixeldefend: Leveraging generative models to understand and defend against adversarial examples. In *International Conference on Learning Representations*, 2017.
- [29] P. Stock and M. Cissé. Convnets and imagenet beyond accuracy: Understanding mistakes and uncovering biases. In *European Conference on Computer Vision*, 2018.
- [30] C. Szegedy, V. Vanhoucke, S. Ioffe, J. Shlens, and Z. Wojna. Rethinking the inception architecture for computer vision. *2016 IEEE Conference on Computer Vision and Pattern Recognition*, pages 2818–2826, 2016.
- [31] C. Szegedy, W. Zaremba, I. Sutskever, J. Bruna, D. Erhan, I. J. Goodfellow, and R. Fergus. Intriguing properties of neural networks. In *International Conference on Learning Representations*, 2014.
- [32] S. Thulasidasan, G. Chennupati, J. A. Bilmes, T. Bhattacharya, and S. E. Michalak. On mixup training: Improved calibration and predictive uncertainty for deep neural networks. In *Advances in Neural Information Processing Systems*, 2019.
- [33] Y. Wen, D. Tran, and J. Ba. Batchensemble: An alternative approach to efficient ensemble and lifelong learning. In *International Conference on Learning Representations*, 2020.
- [34] D. Xin, N. Mayoraz, H. Pham, K. Lakshmanan, and J. R. Anderson. Folding: Why good models sometimes make spurious recommendations. In *Proceedings of the Eleventh ACM Conference on Recommender Systems*, pages 201–209, 2017.
- [35] Y. Yang, G. Zhang, D. Katabi, and Z. Xu. Me-net: Towards effective adversarial robustness with matrix estimation. In *International Conference on Machine Learning*, 2019.

- [36] S. Zagoruyko and N. Komodakis. Wide residual networks. *ArXiv*, abs/1605.07146, 2016.
- [37] H. Zhang, M. Cissé, Y. Dauphin, and D. Lopez-Paz. Mixup: Beyond empirical risk minimization. In *International Conference on Learning Representation*, 2018.
- [38] S. Zheng, Y. Song, T. Leung, and I. Goodfellow. Improving the robustness of deep neural networks via stability training. In *Proceedings of the IEEE Conference on Computer Vision and Pattern Recognition*, pages 4480–4488, 2016.

## A Implementation Details

### A.1 SVHN

We use a simple network architecture with 7 convolutional layers and follow all the training details introduced in [23] for SVHN. This network architecture achieves the state-of-the-art accuracy on SVHN.

### A.2 CIFAR-10

All the experimental results on CIFAR-10 were obtained with a ResNet-29 v2 [10] with a batch size of 256. The network is trained with Adam optimizer [13] for 200 epochs. The initial learning rate is  $10^{-3}$  and decayed down to  $10^{-4}$  after 80 epochs,  $10^{-5}$  after 120 epochs,  $10^{-6}$  after 160 epochs and  $0.5 \times 10^{-6}$  after 180 epochs. We adapted the following data augmentation and training script at [https://keras.io/examples/cifar10\\_resnet/](https://keras.io/examples/cifar10_resnet/). The training mechanism is the same for all the methods that we compare in the main paper. We randomly split the training dataset into training data of 45000 images and 5000 images as the validation set. The test set has 10000 images.

For label smoothing (LS), we sweep the hyperparameter  $\epsilon$  within the range  $[0, 0.1]$  with a step size 0.01 and find that the network has the best calibration performance on the validation set when  $\epsilon = 0.02$ .

For Adaptive Label Smoothing (AdaLS), there is a hyperparameter  $\alpha$  which plays a role as learning rate in the adaptive learning mechanism. We choose hyperparameter  $\alpha$  based on the calibration performance on the validation set. Specifically, we run experiments with  $\alpha \in \{0.005, 0.01, 0.05, 0.1\}$  and find that  $\alpha = 0.05$  achieve the best calibration performance.

Similarly, for Adversarial Robustness based Adaptive Label Smoothing (AR-AdaLS), we choose the hyperparameter  $\alpha$  from the set  $\{0.005, 0.01, 0.05\}$  and empirically set  $\alpha = 0.005$  which has the best calibration performance on the validation set. We use the same hyperparameter  $\alpha = 0.005$  without further tuning for AR-AdaLS of Ensemble.

All the results of ensemble models are obtained via training 5 independent models with random initializations.

### A.3 CIFAR-100

We train a Wide ResNet-28-10 v2 [36] to obtain the state-of-the-art accuracy for CIFAR-100. We adapt the same training details and data augmentation at <https://github.com/google/edward2/blob/master/baselines/cifar/deterministic.py>.

### A.4 ImageNet

All the experiments on ImageNet were obtained via training a ResNet-101 v1 [9] following the training script at <https://github.com/google/edward2/blob/master/baselines/imagenet/deterministic.py>. The network is trained with a batch size of 128 for each TPU core with SGD optimizer for 90 epochs. The input image is normalized (divided by 255) to be within  $[0,1]$ . We randomly divide 50000 validation images into validation set with 25000 images and test set with 25000 images. Note that the same dataset and training mechanisms are used for all the methods that we compare in the main paper.

For Label Smoothing (LS), we sweep the hyperparameter  $\epsilon$  within the range  $[0, 0.1]$  with a step size 0.01 and find that the best calibration performance on the validation set is achieved by setting  $\epsilon = 0.02$ .

For Adaptive Label Smoothing (AdaLS), we sweep the hyperparameter  $\alpha$  in the set  $\{0.005, 0.01, 0.03, 0.05, 0.1\}$  and set it to be  $\alpha = 0.03$  for the best calibration performance on the validation set.

We empirically set  $\alpha = 0.001$  for AR-AdaLS in the first 60 epochs of the training and then increase it to 0.05 for the next 30 epochs. The same hyperparameter  $\alpha$  is used for AR-AdaLS of Ensemble without further tuning.

All the ensemble models are a combination of 5 independent models with random initializations.

### A.5 CW attacks

To compute the adversarial robustness, we construct  $\ell_2$  based CW attacks [4] following the code at [https://github.com/tensorflow/cleverhans/blob/master/cleverhans/attacks/carlini\\_wagner\\_12.py](https://github.com/tensorflow/cleverhans/blob/master/cleverhans/attacks/carlini_wagner_12.py). Specifically, we set the binary search steps to be 3, max iterations to be 500 and learning rate to be 0.005. The generated untargeted CW attacks can achieve 100% success rate for all the datasets that we consider: SVHN, CIFAR-10, CIFAR-100 and ImageNet. We set the number of adversarial robustness training subset and validation subset to be  $R = 10$  respectively.

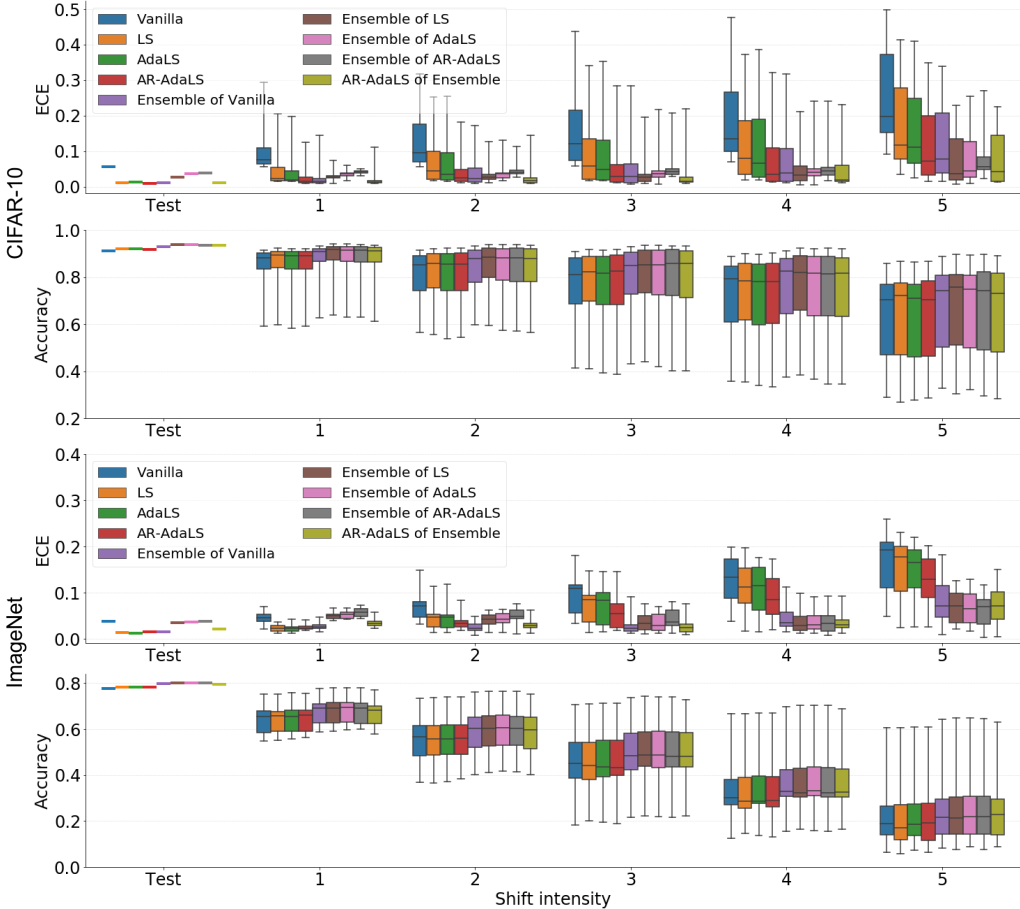


Figure 7: Comparison of ensembled models: ECE and Accuracy on both clean test data and shifted data on CIFAR-10 and ImageNet. For each intensity of shift, we show the results with a box plot summarizing the 25th, 50th, 75th quartiles across 19 types of shift on CIFAR-10-C and 15 types of shift on ImageNet-C. The error bars indicate the *min* and *max* value across different shift types.

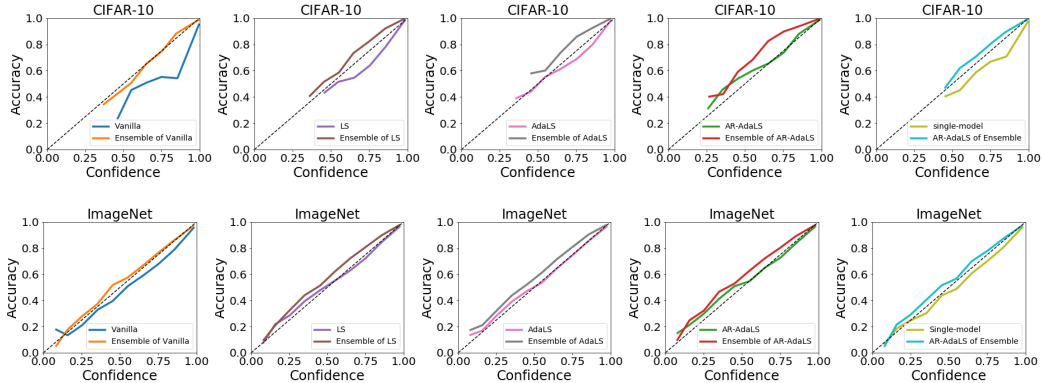


Figure 8: Reliability diagram of accuracy versus confidence of single model and ensemble model on the clean test of CIFAR-10 and ImageNet. The perfect calibrated model should be aligned with the diagonal dotted line (above is under-confident, below is over-confident).

## B Calibration Performance: Additional Results

In Figure 7, we show ECE and accuracy of all the single-models and their corresponding ensembles on the clean test and shifted CIFAR-10 and ImageNet. The high-level conclusion is: 1) all the ensemble models that we compare have similar accuracies, which are higher than single-models. 2) all the ensemble methods perform relatively well for highly shifted data but ensembles of well calibrated models (Ensemble of LS, Ensemble of AdaLS, Ensemble of AR-AdaLS) perform much worse on less shifted and clean test data. 3) AR-AdaLS of Ensemble successfully learns to adaptively adjust its smoothing level to keep the ensemble well calibrated on both clean and shifted dataset.

Figure 8 is to validate the observation that naive ensembling of a single model can improve calibration on highly shifted data where single-model is over-confident but can harm calibration on clean test data where single model is well calibrated. As shown in Figure 8, we can see that if the single-model is over-confident (Vanilla), Ensemble of Vanilla greatly improves the model’s calibration. However, when the single model is well-calibrated (LS, AdaLS, AR-AdaLS), naive ensembling of these models leads to an under-confident model with a worse calibration performance. In contrast, AR-AdaLS of Ensemble successfully avoids this issue by adaptively smoothing the training labels according to adversarial robustness of training data.

## C Numerical Results

We report the mean of variance and mean of ECE across 19 types of shift for CIFAR-10-C and 15 types of shift for ImageNet-C in Table 2 and Table 3. We can see that AR-AdaLS achieves the best performance in model’s calibration (the smallest ECE) and stability (the smallest variance) among all the single-model based methods on the corrupted datasets. For the ensemble models, our proposed AR-AdaLS of Ensemble also achieves the best calibration performance on the corrupted datasets.

Table 2: Mean of variance ( $\times 10^{-2}$ ) across 19 types of shift for CIFAR-10-C and 15 types of shift for ImageNet-C. The best model is shown in **bold**.

Dataset	CIFAR-10-C					ImageNet-C				
	1	2	3	4	5	1	2	3	4	5
Vanilla	7.85	9.69	11.2	13.1	16.0	5.28	6.39	7.37	8.23	8.29
LS	5.54	6.95	8.11	9.65	11.8	4.86	5.84	6.78	7.55	7.41
AdaLS	5.47	6.87	7.95	9.44	11.5	4.79	5.77	6.66	7.51	7.56
AR-AdaLS	<b>4.21</b>	<b>5.06</b>	<b>5.73</b>	<b>6.66</b>	<b>8.24</b>	<b>4.53</b>	<b>5.49</b>	<b>6.12</b>	<b>6.76</b>	<b>6.66</b>

Table 3: Mean of ECE ( $\times 10^{-2}$ ) across 19 types of shift for CIFAR-10-C and 15 types of shift for ImageNet-C. The best single model and ensemble model are shown in **bold** respectively.

Dataset	CIFAR-10-C					ImageNet-C				
Shift Intensity	1	2	3	4	5	1	2	3	4	5
Vanilla	9.59	12.9	15.6	19.5	25.7	4.67	6.94	9.60	13.2	16.6
LS	4.45	7.06	9.15	12.1	17.5	2.38	4.62	7.39	11.4	15.1
AdaLS	4.06	6.65	8.85	11.7	16.5	<b>2.37</b>	4.48	7.18	11.1	14.6
AR-AdaLS	<b>2.57</b>	<b>4.09</b>	<b>5.64</b>	<b>7.85</b>	<b>11.9</b>	2.44	<b>3.58</b>	<b>5.80</b>	<b>9.33</b>	<b>12.9</b>
Ensemble of Vanilla	2.47	4.13	5.73	8.03	12.1	2.77	<b>2.51</b>	2.87	4.64	8.26
Ensemble of LS	2.77	3.24	3.96	5.20	7.85	4.96	4.18	3.65	3.65	6.94
Ensemble of AdaLS	3.48	3.74	4.86	5.95	7.74	5.20	4.36	3.61	3.74	6.92
Ensemble of AR-AdaLS	4.23	4.52	5.23	5.68	<b>7.68</b>	5.76	5.23	4.51	3.69	<b>6.33</b>
AR-AdaLS of Ensemble	<b>1.97</b>	<b>2.98</b>	<b>3.91</b>	<b>5.38</b>	7.98	3.41	3.03	<b>2.84</b>	<b>3.61</b>	7.03